Functional interplay between LIS1, NDE1 and NDEL1 in dynein-dependent organelle positioning

Connie Lam, Maïlys A. S. Vergnolle, Lisa Thorpe, Philip G. Woodman*,‡ and Victoria J. Allan*,‡

Faculty of Life Sciences, University of Manchester, Manchester, M13 9PT, UK

*These authors contributed equally to this work

‡Authors for correspondence (philip.woodman@manchester.ac.uk; viki.allan@manchester.ac.uk)

Accepted 9 October 2009
Journal of Cell Science 123, 202-212 Published by The Company of Biologists 2010
doi:10.1242/jcs.059337

Summary

LIS1, NDE1 and NDEL1 modulate cytoplasmic dynein function in several cellular contexts. However, evidence that they regulate dynein-dependent organelle positioning is limited. Here, we show that depletion of NDE1 or NDEL1 alone profoundly affected the organisation of the Golgi complex but did not cause it to disperse, and slightly affected the position of endocytic compartments. However, striking dispersal of organelles was observed when both NDE1 and NDEL1 were depleted. A substantial portion of NDE1 and NDEL1 is membrane associated, and depletion of these proteins led to complete loss of dynein from membranes. Knockdown of LIS1 also caused the Golgi complex to fragment and disperse throughout the cell, and caused endocytic compartments to relocalise to the periphery. Depletion of LIS1, which is primarily cytosolic, led to partial loss of membrane-associated dynein, without affecting NDE1 and NDEL1. These data suggest that NDE1 and NDEL1 act upstream of LIS1 in dynein recruitment, and/or activation, on the membrane. Consistent with this hypothesis, expression of exogenous NDE1 or NDEL1 rescued the effects of LIS1 depletion on Golgi organisation, whereas LIS1 was only partially effective at rescuing the loss of NDE1 and NDEL1.

Key words: LIS1, dynein, Golgi, Endosomes, Microtubules

Introduction

Cytoplasmic dynein 1 is a minus-end-directed microtubule motor that is required for a wide range of activities involving movement or anchoring of cellular structures (Vallee et al., 2004). These activities include separation of chromosomes during mitosis, cell migration, and the movement and localisation of substrates such as mRNAs, signalling complexes and membrane organelles. To understand how dynein function over such a diverse range of activities is regulated, much attention has focussed on the composition of the dynein motor complex and the roles of accessory proteins.

Dynein can be purified as a 1.6 MDa complex. This contains two copies of a motor subunit (dynein heavy chain; DHC), each of which comprises an AAA ATPase region involved in force generation and a stem region that connects the ATPase to the remaining, regulatory and cargo-binding subunits of the dynein complex. These subunits include dynein intermediate chain (DIC), dynein light intermediate chain (DLIC), and dynein light chains (DLCs) (Pfister et al., 2006). Dynein engages several accessory proteins or protein complexes, which might regulate its motor and/or cargo-binding activities. The best characterised of these is dynactin, a multiprotein complex that is almost universally associated with dynein-dependent functions (Schroer, 2004). More recently, several additional dynein-interacting proteins have been identified using a screen for *Aspergillus nidulans* mutants that are defective for nuclear distribution. These include NudF (Xiang et al., 1995) and NudE (Efimov and Morris, 2000), the higher eukaryote counterparts of which are Lissencephaly1 (LIS1) and NDE1, respectively. An NDE1-related protein, NDEL1 (also referred to as NudEL) has also been identified (Niethammer et al., 2000; Sasaki et al., 2000). LIS1 interacts directly with DHC via sites on the first AAA domain and the stem region (Sasaki et al., 2000; Tai et al., 2002), with DIC (Tai et al., 2002), and with the p50 subunit of dynactin (Tai et al., 2002). NDEL1 and NDE1 also bind to dynein. However, the mode of binding might not be conserved here, because NDEL1 has been reported to bind HC (Sasaki et al., 2000), whereas NDE1 binds to DIC and the LC8 isoform of DLC (Stehman et al., 2007). In addition, NDE1 (Efimov and Morris, 2000; Feng et al., 2000) and NDEL1 (Derewenda et al., 2007; Niethammer et al., 2000; Sasaki et al., 2000) bind to LIS1 directly, and to each other (Bradshaw et al., 2009). There are currently two models to explain how these effectors modulate dynein function. They might regulate dynein motor activity directly (Mesngon et al., 2006; Yamada et al., 2008), or they might have a role in targeting dynein to cargoes (Liang et al., 2007; Vergnolle and Taylor, 2007).

LIS1, NDE1 and NDEL1 have been implicated in many dynein-mediated activities, including cell migration, (Ding et al., 2009; Dujardin et al., 2003; Feng and Walsh, 2004; Kholmanskikh et al., 2003; Sasaki et al., 2005; Shu et al., 2004; Tanaka et al., 2004; Tsai et al., 2007; Tsai et al., 2005), embryonic pronuclear migration (Cockell et al., 2004; Payne et al., 2003; Swan et al., 1999), targeting of dynein onto cortical microtubules (Li et al., 2005a; Sheeman et al., 2003) and correct functioning of the mitotic spindle (Ding et al., 2009; Faulkner et al., 2000; Feng and Walsh, 2004; Liang et al., 2007; Mori et al., 2007; Siller et al., 2005; Tai et al., 2002; Tsai et al., 2005; Vergnolle and Taylor, 2007; Yan et al., 2003; Yingling et al., 2008). Mutations in or haplo-insufficiency of mammalian LIS1 are associated with Type 1 Lissencephaly, a broad-spectrum disorder resulting from defects in cortical neuronal progenitor cell division and neuronal migration (Gambello et al., 2003; Hirotsune et al., 1998; Lo Nigro et al., 1997; Vallee and Tsai, 2006).

In contrast to these events, the involvement of LIS1 in the dynein-dependent movement and positioning of cytoplasmic organelles is controversial. In several studies, interventions that inhibited other LIS1-dependent activities did not affect membrane organisation (Dujardin et al., 2003; Faulkner et al., 2000; Tai et al., 2002). Elsewhere, mild (Sasaki et al., 2000; Smith et al., 2000) or more severe (Ding et al., 2009; Kondratova et al., 2005; Rehberg et al., 2005) effects on Golgi positioning were seen upon LIS1 reduction,

Journal of Cell Science

but these might have been secondary to the profound changes in microtubule architecture that were also reported. Drosophila LIS1$^{-/-}$ neurons display defects in axonal transport, although the phenotype differs somewhat from DHC mutants (Liu et al., 2000). Overexpression of LIS1 has been reported to leave the Golgi complex position unchanged (Faulkner et al., 2000), more compact (Smith et al., 2000) or dispersed (Kondratova et al., 2005). There is stronger evidence for an involvement of NDEL1 in membrane positioning, because overexpression of LIS1- or dynein-binding NDEL1 mutants alters the position and centripetal movement of a range of organelles and membrane cargo (Liang et al., 2004). Reduction in NDEL1 expression affects the positioning of the Golgi complex (Liang et al., 2004; Sasaki et al., 2005) and lysosomes (Guo et al., 2006), but it is possible that changes in cytoskeletal organisation also contribute to these phenotypes (Sasaki et al., 2005). In addition, the relationship between NDE1 and NDEL1 in controlling organelle positioning has not been explored. This paper uses a systematic, RNAi-based approach to identify the contributions of LIS1, NDE1 and NDEL1 to membrane positioning unambiguously and to explore the functional relationships between each of them.

Results

LIS1 is essential for maintaining organelle positioning

The cellular positioning of the Golgi complex and endosomal compartments are dependent on dynein. However, the requirement for LIS1 in these functions is controversial, despite its involvement in other dynein-dependent cellular processes. We found that simple overexpression of GFP-LIS1 in HeLaM cells did not cause Golgi complex dispersal (a typical phenotype seen following disruption of dynein activity), in agreement with some studies (Dujardin et al., 2003; Faulkner et al., 2000; Tai et al., 2002), but in contrast to other work (Kondratova et al., 2005; Sasaki et al., 2000). Instead, the Golgi became somewhat more compact compared with control cells (Fig. 1A; see supplementary material Table S1 for statistical analysis), as reported before (Smith et al., 2000). An alternative way of looking at LIS1 function is to deplete the endogenous protein. LIS1 expression was prevented using a previously characterised siRNA oligonucleotide (Tsai et al., 2005), leading to almost complete removal of LIS1 protein (Fig. 1B). The time taken for LIS1-depleted cells to progress through mitosis increased to 260% compared with that in control cells (P<0.0001; Table 1). This is consistent with the delay in mitosis caused by microinjection of anti-LIS1 antibody and the twofold increase in mitotic index observed upon depletion of LIS1 (Faulkner et al., 2000). In addition, many LIS1-depleted interphase cells displayed micronuclei (supplementary material Fig. S1A), indicating a high incidence of aberrant mitosis (Table 2), as observed previously (Faulkner et al., 2000). These data demonstrate a functional depletion of LIS1 protein.

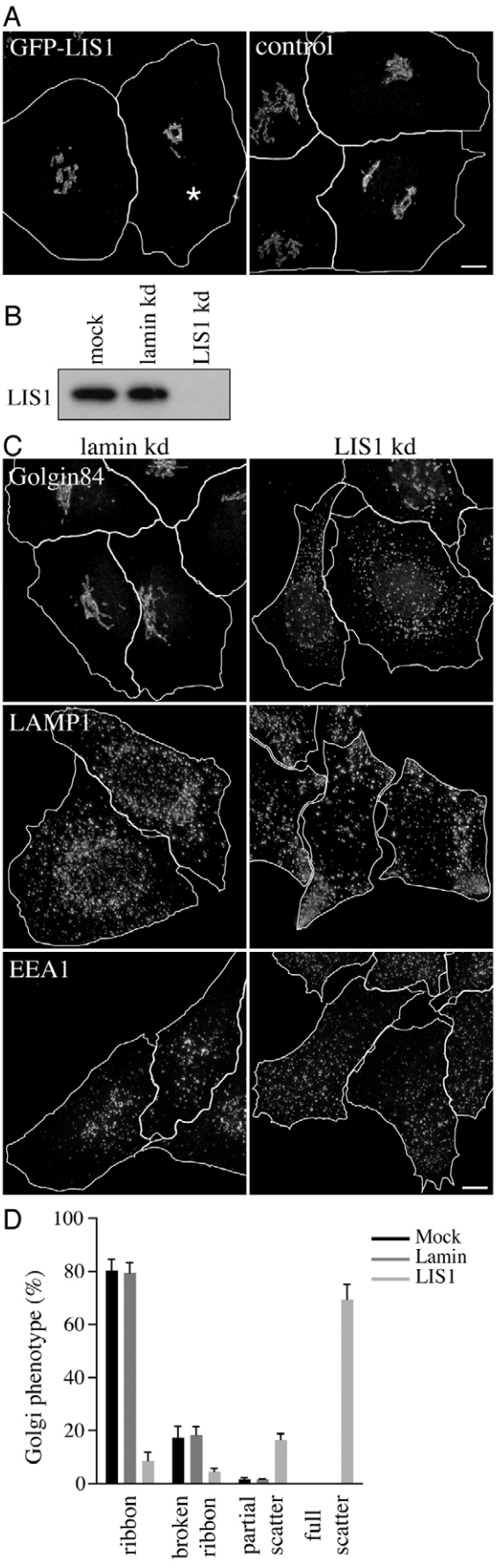

Fig. 1. LIS1 is essential for organelle positioning. (**A**) Cells transiently transfected with GFP-LIS1 (left) or untreated (right), were fixed, and immunostained for golgin84 (transfected cells are indicated by asterisks). Scale bar: 10 µm. (**B**) Cells were mock treated or depleted of lamin A/C or LIS1, lysed, and equal amounts of protein from each lysate were immunoblotted accordingly. (**C**) Cells depleted of lamin A/C or LIS1 were immunostained for golgin84, LAMP-1 or EEA1. Scale bar: 10 µm. (**D**) Cells treated with siRNA were scored for Golgi phenotypes as indicated (see supplementary material Fig. S2 for examples of each phenotype). Values are expressed as mean percentages ± s.e.m. from three independent experiments. 500 cells were counted for each condition per experiment. Statistical analysis is provided in supplementary material Table S2.

Table 1. Duration of mitosis in siRNA-treated cells*

RNAi condition	Cell number	Mitosis duration (minutes ± s.d.)	*P*-value
Mock	262	44.3±14.3	–
Lamin	262	44.2±13.5	0.197
LIS1	262	117.1±100.2	0.0001
NDE1	262	87.2±53.9	0.0001
NDEL1	262	45.0±11.8	0.875
NDE1+NDEL1	243	98.8±59.1	0.0001

*Cells were imaged by time-lapse microscopy 72 hours after RNAi, and the length of mitosis calculated. A total of up to 262 cells were selected at random from three separate experiments. Values are means ± s.d.; *P*-values from two-tailed Mann-Whitney analysis are shown.

Upon depletion of LIS1, the positioning of the Golgi-tethering factor, golgin84 (Diao et al., 2003), was severely affected. In control-treated cells (data not shown) or cells treated with siRNA against an unrelated protein, lamin A/C, (Fig. 1C), the Golgi complex was localised to the perinuclear region and was organised into a series of interconnected structures. In LIS1-depleted cells, these were replaced by small fragments of golgin84-positive membrane that were dispersed throughout the cell (Fig. 1C). Localisation of another golgin, GM130 (Puthenveedu et al., 2006), was similarly affected upon loss of LIS1 (data not shown). In addition, Golgi positioning was similarly affected in cells depleted of LIS1 using an independent, 'SmartPool' combination of oligonucleotides (supplementary material Fig. S1A). To provide a more quantitative assessment of the degree of Golgi dispersal, cells were selected into one of four categories based on their distribution of golgin84 staining (see supplementary material Fig. S2 for details). Of cells treated with *LIS1* siRNA, 70% showed a severe defect in Golgi positioning, with highly scattered small fragments. This phenotype was never observed in untreated cells or cells treated with siRNA against lamin A/C (Fig. 1D; see supplementary material Table S2 for statistical analysis). In addition, 17% of LIS1-depleted cells exhibited an intermediate defect in Golgi positioning (partial scatter), in which golgin84 staining was highly fragmented, but remained localised fairly centrally within the cell. This phenotype was rarely seen in control cells.

The importance of LIS1 for organelle positioning is not confined to the Golgi complex. LAMP-1 is an integral membrane marker for lysosomes and late endosomes. LAMP-1 redistributed from a mainly perinuclear location in control-treated (data not shown) or lamin-A/C-depleted cells (Fig. 1C) towards the cell periphery when LIS1 was depleted (Fig. 1C). In lamin-A/C-depleted cells, the early endosome marker, EEA1, varied somewhat in positioning, but in most cells some EEA1 concentrated in larger structures towards the cell centre (Fig. 1C). EEA1 staining became spread more evenly throughout the cell, or became dispersed towards the cell periphery upon loss of LIS1 (Fig. 1C). The distribution of transferrin receptor (TfR), a marker for the recycling endosome, was also affected (supplementary material Fig. S3). In control HeLaM cells, TfR was most concentrated in the perinuclear region, although it was also found at the cell periphery. The perinuclear concentration of TfR was lost when LIS1 was depleted, and instead TfR labelling was somewhat stronger at the cell periphery.

To identify whether these effects resulted specifically from loss of LIS1, siRNA-treated cells were transiently transfected with human GFP-LIS1 incorporating silent mutations making it resistant to RNAi (GFP-LIS1*). This substantially restored the positioning of golgin84, LAMP1 and EEA1 towards normal positions (Fig. 2A). Indeed, quantitative analysis showed that transfection of GFP-LIS1* into both siRNA-depleted or mock-depleted cells often generated a more tightly focussed and compact Golgi complex than seen in untransfected cells (Fig. 2B, see supplementary material Table S2 for statistical analysis), as was seen when LIS1 was overexpressed in control cells (Fig. 1A, supplementary material Table S1). Therefore, the structure and position of the Golgi complex correlates with levels of LIS1.

Several missense mutations have been mapped to the *LIS1* gene that result in lissencephaly in heterozygous individuals (Cardoso et al., 2000; Lo Nigro et al., 1997). Compared with transient expression of wild-type LIS1*, transient expression of LIS1*(F31S), which is mutated at the LIS1 dimerisation interface (Tarricone et al., 2004), or LIS1*(H149R) and LIS1*(S169P), mutations that map to the β-propeller, effector-binding portion of LIS1 (Tarricone et al., 2004), did not restore normal positioning of the Golgi complex to LIS1-depleted cells (Fig. 2B and supplementary material Fig. S4). Hence, disease-associated LIS1 mutants fail to support normal Golgi positioning.

Both NDE1 and NDEL1 are important for maintaining organelle positioning

Previous studies have shown that RNAi-mediated depletion of NDEL1 causes scattering of the Golgi complex, but the interpretation of these experiments was complicated by the fact that NDE1 levels were also reduced under these conditions (Liang et al., 2004). Neurons with reduced NDEL1 expression displayed some defect in the distribution of the COPI coatomer subunit βCOP, which is used as a Golgi complex marker (Sasaki et al., 2005), although in this case NDE1 expression was maintained at normal levels. To determine whether both NDEL1 and NDE1 are essential for organelle organisation and positioning, or whether they might be redundant in these respects, cells were treated with siRNA specific for each protein, either individually or in combination. Treatment with *NDEL1* or *NDE1* siRNA reduced the levels of the respective protein specifically (Fig. 3A). The duration of mitosis increased by 223% after depletion of both NDE1 and NDEL1 ($P<0.0001$; Table 1). It increased by 197% in cells depleted of NDE1 alone ($P<0.0001$;

Table 2. Nuclear phenotypes of siRNA-treated cells*

RNAi condition	Cell number	% Normal	% With micronuclei	% Binucleate	% Multinucleate
Mock	311	98.1	0.3	1.6	0
Lamin	242	94.6	1.7	3.7	0
LIS1	257	77.4	19.5	3.1	0
NDE1	268	66.7	22.4	7.5	3.4
NDEL1	324	95.4	3.1	1.5	0
NDE1+NDEL1	267	71.2	20.6	7.1	1.1

*siRNA-treated cells were fixed after 72 hours and stained with DAPI. The indicated number of cells was counted from two independent experiments, and phenotypes scored as described. Values are expressed as mean percentages of the total cell number. The level of apoptosis was not affected by any treatment.

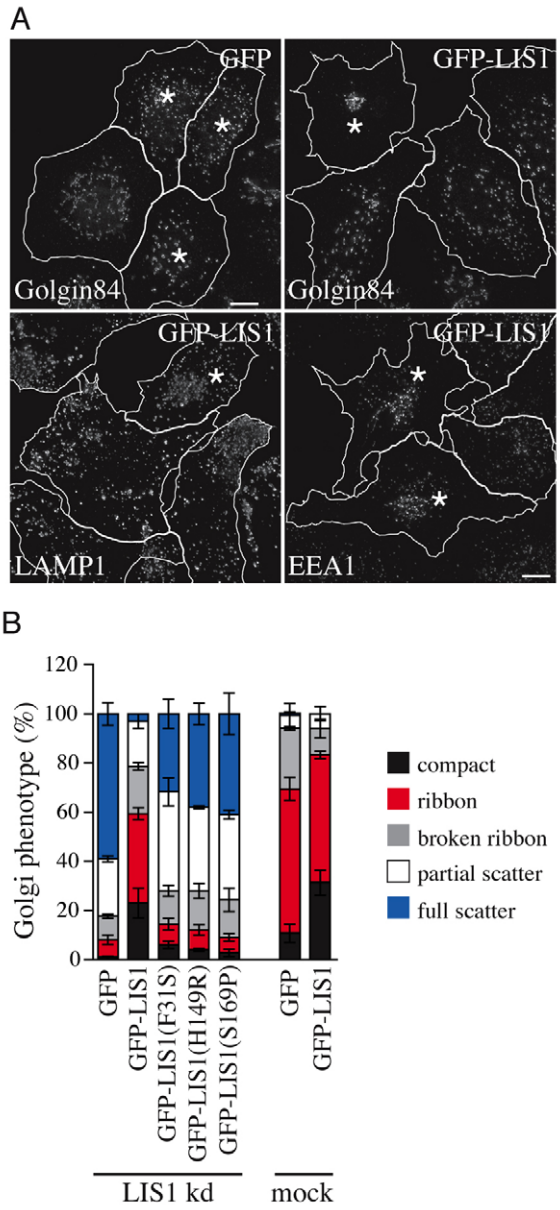

Fig. 2. Expression of GFP-LIS1 restores organelle positioning to LIS1-depleted cells. (**A**) LIS1-depleted cells were transfected with GFP or GFP-LIS1* and stained for golgin84, LAMP-1 or EEA1 (transfected cells are indicated by asterisks). Scale bar: 10 μm. (**B**) LIS1-depleted cells (left columns) or mock-treated cells (right columns) were transfected with GFP, GFP-LIS1*, GFP-LIS1*(F31S), GFP-LIS1*(H149R) or GFP-LIS1*(S169P), as indicated, and stained for golgin84. Cells were scored for Golgi phenotypes as indicated. Values are expressed as mean percentages ± s.e.m. from four independent experiments. 100 cells were counted for each transfection per experiment. Statistical analysis is provided in supplementary material Table S2.

Table 1) and did not increase after depletion of NDEL1 alone (Table 1). These data are consistent with the conclusions of previous studies showing that NDE1 has an important role in mitotic progression in HeLa cells (Vergnolle and Taylor, 2007) and that NDE1-knockout mice display a reduction in mitosis in the ventricular zone (Feng and Walsh, 2004), but further indicate that loss of both NDE1 and NDEL1 might have a greater effect on mitosis than loss of NDE1 alone.

Loss of NDE1 affected the structure and positioning of the Golgi complex, with many cells displaying more fragmented golgin84 labelling. This consisted either of golgin84 in threads that had separated from each other, but remained close to the cell centre, or somewhat smaller fragments that were also mainly centrally located (Fig. 3B,C). Dispersal of golgin84 labelling into small, dispersed fragments, as found after LIS1 depletion, was rarely observed. Transfection with a separate siRNA oligonucleotide against *NDE1* generated a similar phenotype (supplementary material Fig. S1B). This second oligonucleotide generated more pronounced Golgi scattering when used at higher concentrations, but this was accompanied by extensive cell death and loss of ~50% dynein intermediate chain (data not shown). In cells depleted of NDEL1 alone, although the Golgi phenotype ranged from short threads to widely scattered fragments, ~80% of cells displayed an intermediate phenotype of partially scattered fragments (Fig. 3B,C). Strikingly, when both NDEL1 and NDE1 were depleted, the Golgi complex became scattered throughout the cytoplasm in ~70% of cells, with a severity of defect very similar to that observed after LIS1 depletion (Fig. 3B,C; supplementary material Fig. S1B). Another dynein regulator, ZW10, is also required to maintain the structure of the Golgi complex (Hirose et al., 2004; Sun et al., 2007). In cells depleted of ZW10, the Golgi complex fragmented into very short tubules that remained in a patch close to the cell centre (supplementary material Fig. S1B), a phenotype that clearly differed from those observed upon depletion of LIS1, NDE1 or NDEL1.

Depletion of NDEL1 and NDE1 also had a combinatorial effect on the positioning of lysosomes and early endosomes. LAMP1 distribution was somewhat affected by loss of NDE1, or by loss of NDEL1, as previously reported (Guo et al., 2006). However, LAMP1 became highly dispersed to the cell periphery when both NDE1 and NDEL1 were depleted (Fig. 3B). EEA1 localisation was slightly altered compared with control cells upon NDEL1 depletion, or upon NDE1 depletion. However, it became substantially dispersed when both NDEL1 and NDE1 were depleted (Fig. 3B). TfR distribution was also affected in these cells, and appeared similar to that in cells depleted of LIS1 (supplementary material Fig. S3).

The functional relationship between LIS1, NDE1 and NDEL1 in maintenance of organelle positioning

Our data suggest that both NDE1 and NDEL1 participate in dynein-dependent positioning of organelles, although their roles in other aspects of cell physiology might be distinct. To further address whether their functions in supporting organelle positioning are equivalent, cells depleted of NDEL1, NDE1, or a combination of the two, were transfected with RNAi-resistant mutants of GFP-NDEL1 (GFP-NDEL1*) or GFP-NDE1 (GFP-NDE1*). Since high levels of NDEL1 or NDE1 overexpression lead to Golgi scattering (data not shown and Liang et al., 2004) and disruption of the microtubule network (Feng and Walsh, 2004), we first carefully titrated the levels of GFP-NDEL1* and GFP-NDE1* plasmids used in transfections to avoid these dominant-negative effects. The Golgi-positioning phenotypes of cells depleted of NDEL1, NDE1, or NDEL1 plus NDE1 were effectively reversed when either GFP-NDEL1* or GFP-NDE1* were expressed (Fig. 4; see supplementary material Table S2 for statistical analysis), suggesting that the functions of these proteins are redundant in this respect. No further rescue was observed upon combined transfection with GFP-NDEL1* and Myc-NDE1* (data not shown). Interestingly, expression of low levels of GFP-NDEL1* or GFP-NDE1* led to a more compact Golgi

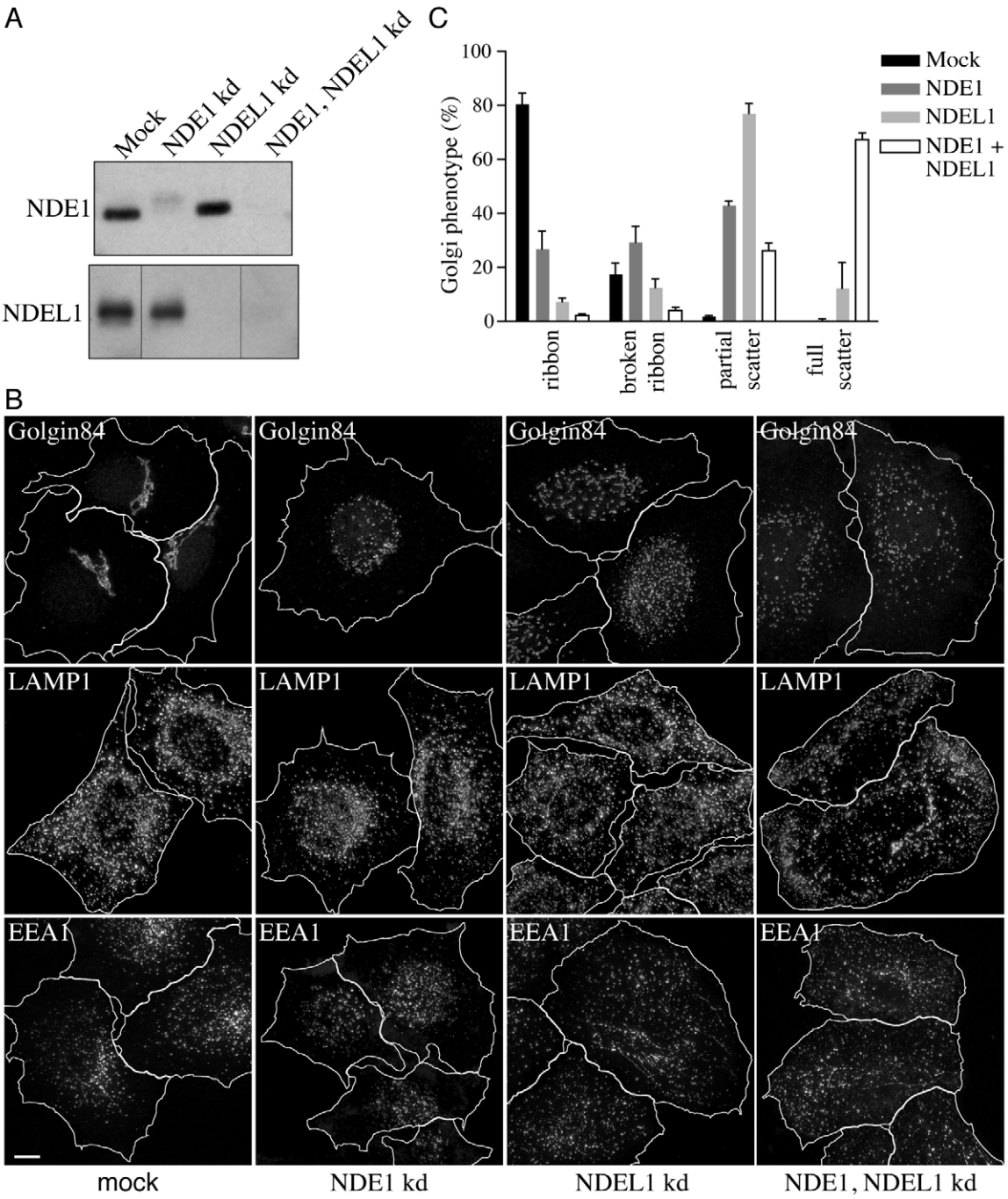

Fig. 3. NDE1 and NDEL1 are essential for organelle positioning. (**A**) Cells were mock treated, depleted (kd) of NDE1, NDEL1 or both NDE1 and NDEL1, lysed, and immunoblotted. Note that a band migrating just above the position of NDE1 is sometimes seen in NDE1-depleted lysates. (**B**) Cells depleted as indicated were immunostained for golgin84, LAMP-1 or EEA1. Scale bar: 10 μm. (**C**) Cells treated with siRNA were scored for Golgi phenotypes, as indicated. Values are expressed as mean percentages ± s.e.m. from three independent experiments. 500 cells were counted for each condition per experiment. Note that the values for mock-treated control cells are also shown in Fig. 1.

organisation in 40-50% of cells, compared with ~10% of mock-depleted cells (Fig. 4C; see supplementary material Table S1 for statistical analysis). The positioning of early endosomes and lysosomes, which was altered in NDE1/NDEL1-depleted cells, was rescued by expressing GFP-NDEL1* or GFP-NDE1* (Fig. 5).

When cells depleted of LIS1 were transfected with either GFP-NDEL1* or GFP-NDE1*, this resulted in a significant reduction in the severity of the Golgi-dispersal phenotype compared with cells transfected with a GFP control (Fig. 6; see supplementary material Table S1 for statistical analysis). Broadly similar findings were seen for distribution of both LAMP-1 and EEA1 when GFP-NDEL1* was expressed (supplementary material Fig. S5). By contrast, the phenotype displayed by cells depleted of both NDE1 and NDEL1 was only slightly reduced by overexpression of GFP-LIS1*, with

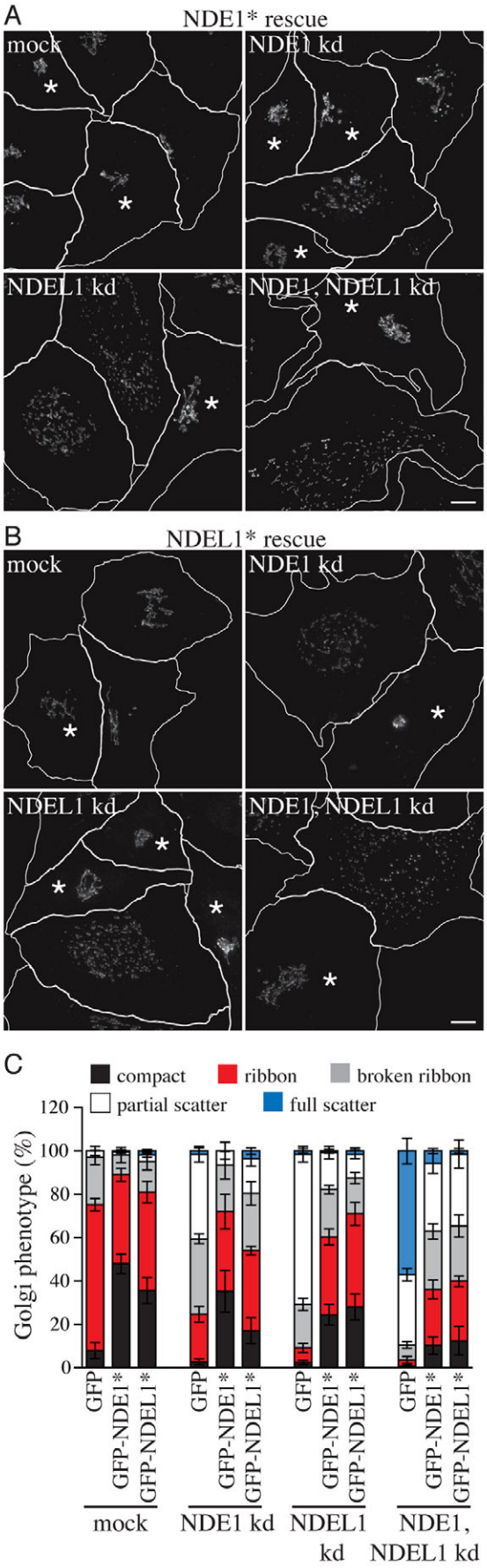

Fig. 4. NDE1 or NDEL1 restore Golgi positioning to NDE1- and NDEL1-depleted cells. Cells depleted of one or both of NDE1 and NDEL1, or subjected to mock depletion, were transiently transfected with GFP-NDE1* (**A**) or GFP-NDEL1* (**B**) and immunostained for golgin84 (transfected cells are indicated by asterisks). Transfected cells are indicated by asterisks. Scale bars: 10 µm. (**C**) Cells depleted as indicated were transfected with GFP, GFP-NDE1* or GFP-NDEL1*, and stained for golgin84. Cells were scored for Golgi phenotypes as indicated in Fig. 2. Values are expressed as mean percentages ± s.e.m. from four independent experiments. 100 cells were counted for each transfection per experiment. Statistical analysis is provided in supplementary material Table S2.

a shift from full to partial scattering, but little reassembly of Golgi ribbons (Fig. 6).

Loss of LIS1, or NDE1 and NDEL1, impairs dynein recruitment to membranes

The phenotypes generated by LIS1, or NDE1 and NDEL1, depletion suggest that dynein activity during membrane positioning is impaired in these cells. To test whether RNAi reduced the stability of dynein and/or dynactin, cells were analysed by western blot for dynein intermediate chain (DIC) and p150^{Glued}, which are components of the dynein and dynactin complexes, respectively. The levels of both proteins were unaffected (Fig. 7A). In addition, all DIC remained part of a high molecular weight dynein complex in siRNA-depleted cells, as assessed by sedimentation on sucrose gradients (Fig. 7B). However, loss of LIS1 substantially reduced the amount of DIC that co-fractionated with membranes, whereas no membrane-associated DIC was detected at all following depletion of both NDE1 and NDEL1 (Fig. 7C). Interestingly, although dynactin and LIS1 were predominantly cytosolic in all conditions, both NDE1 and NDEL1 were plentiful in the membrane fraction, and their levels were not altered by LIS1 depletion (Fig. 7D). Hence,

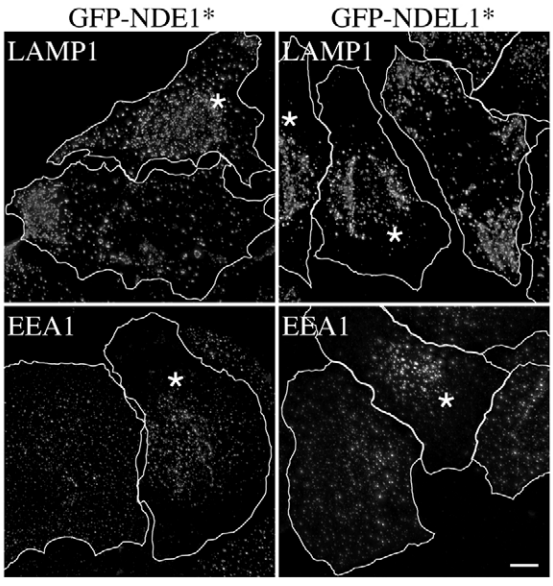

Fig. 5. NDE1 or NDEL1 restore endosome and lysosome positioning to NDE1- and NDEL1-depleted cells. Cells depleted of NDE1 and NDEL1 were transiently transfected with GFP-NDE1* or GFP-NDEL1* and immunostained for LAMP1 or EEA1 (transfected cells are indicated by asterisks). Scale bar: 10 µm.

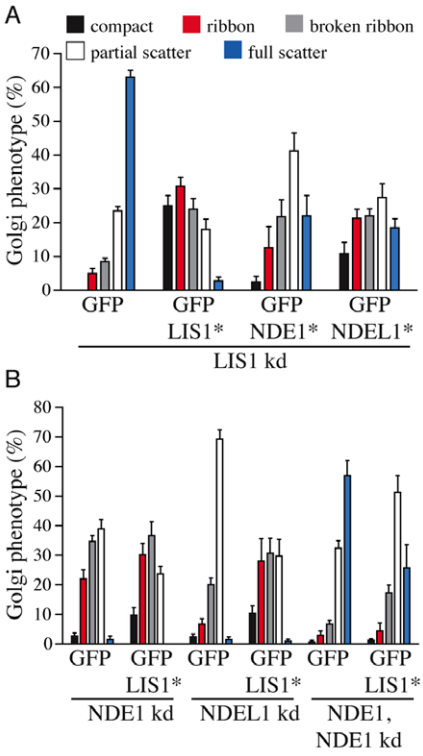

Fig. 6. NDE1 and NDEL1 compensate for loss of LIS1 to support organelle positioning. (**A**) Cells depleted of LIS1 were transfected with GFP, GFP-LIS1*, GFP-NDE1* or GFP-NDEL1*, then stained for golgin84. Cells were scored for Golgi phenotypes as indicated in Fig. 2. Values are expressed as mean percentages ± s.e.m. from four independent experiments. 100 cells were counted for each transfection per experiment. Statistical analysis is provided in supplementary material Table S2. (**B**) As for A, but cells depleted for NDE1, NDEL1 or a combination of NDE1 and NDEL1 were transfected with either GFP or GFP-LIS1*.

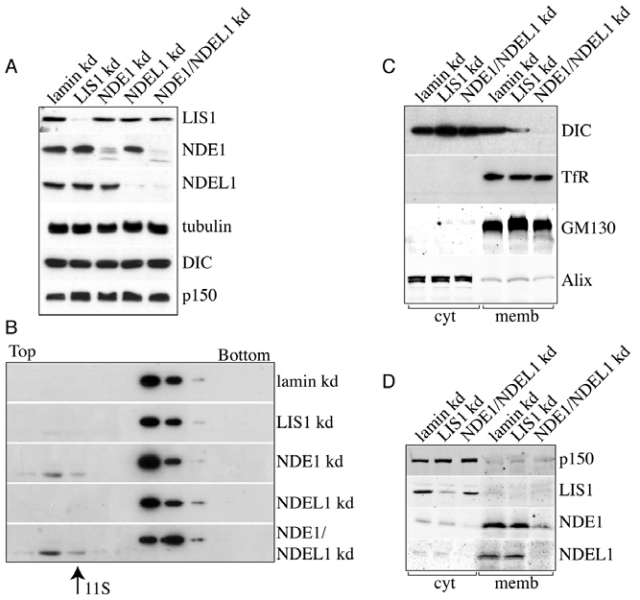

Fig. 7. Loss of LIS1, or NDE1 and NDEL1 does not affect dynein complex integrity but impairs dynein recruitment to membranes. (**A**) Cells were depleted (kd) as indicated, then western blotted for LIS1, NDE1 and NDEL1, or for tubulin, dynein intermediate chain (DIC), and the p150^{Glued} subunit of dynactin. (**B**) Detergent lysates were prepared from cells depleted as indicated, then run on 5-20% sucrose gradients and western blotted for the presence of dynein intermediate chain. The top and bottom of the gradients are indicated, as well as the migration of catalase standard (11S). A non-specific band in fractions 2-4 is seen in some samples. (**C**) Cells depleted as indicated were homogenised and fractionated into membranes and cytosol by centrifugation. Equal protein samples from each cell preparation were western blotted for DIC, transferrin receptor (TfR) and GM130 as membrane markers, or Alix as a soluble marker. Loading for membranes was approximately 10 times higher than for cytosol in terms of cell equivalents. (**D**) As for C, except fractions were immunoblotted for p150, LIS1, NDE1 or NDEL1.

LIS1 and NDE1 plus NDEL1 are essential for efficient dynein binding to membranes, whereas LIS1 is not required for NDE1 or NDEL1 membrane association. Note that a minor loss of LIS1 might occur in cells depleted of NDE1 or NDEL1 (Fig. 7A).

The effects on organelle positioning caused by loss of LIS1, NDE1 and NDEL1 cannot be attributed to changes in cytoskeleton structure or dynamics

LIS1 and NDEL1 help to stabilise cortical microtubules via a mechanism that involves CLIP170, dynactin and dynein (Coquelle et al., 2002; Li et al., 2005a; Sheeman et al., 2003; Yingling et al., 2008). In addition, interfering with LIS1 or NDE1 and NDEL1 function in some systems has been shown to alter microtubule distribution profoundly (Ding et al., 2009; Guo et al., 2006; Rehberg et al., 2005; Sasaki et al., 2005; Sasaki et al., 2000; Smith et al., 2000). To address whether gross changes in microtubule organisation could account for the redistribution of organelles observed upon depletion of LIS1 or NDE1 and NDEL1, siRNA-depleted cells were stained for microtubules and for golgin84, and scored for a range of interphase microtubule organisation phenotypes (supplementary material Fig. S6) and for Golgi positioning. As shown in supplementary material Table S3, depletion of LIS1, NDE1 and NDEL1 had only minor effects on microtubule organisation within a small proportion of cells, giving phenotypes that are broadly consistent with previous findings. Although the whorls of microtubules previously identified upon alteration of LIS1 levels (Rehberg et al., 2005; Smith et al., 2000) were observed in 7% of LIS1-depleted cells, this rearrangement was clearly independent of the changes in Golgi complex distribution seen in over 85% of LIS1-depleted cells (data not shown; see also Fig. 1D).

LIS1 and NDEL1 influence actin organisation and dynamics by indirectly regulating Rho GTPases (Kholmanskikh et al., 2003; Kholmanskikh et al., 2006; Rehberg et al., 2005; Shen et al., 2008). Although we observed alterations in actin organisation in LIS1 and NDE1-depleted cells, the phenotypes were not conserved between different LIS1 and NDE1 oligonucleotides (data not shown). Knockdown of NDEL1 using two distinct oligonucleotides caused the majority of cells to display prominent stress fibres, and they also lacked filopodia, whereas untreated HeLaM cells displayed a much wider range of actin distribution (data not shown). Hence, although recent evidence suggests a role for actin in the positioning of the Golgi complex (Campellone et al., 2008) and lysosomes (Loubery et al., 2008), our data show that there is no consistency between actin organisation and Golgi positioning, so that changes in actin distribution cannot account for the alterations in Golgi distribution. In support of this conclusion, overexpression of the dynactin subunit p50 caused substantial dispersal of the Golgi

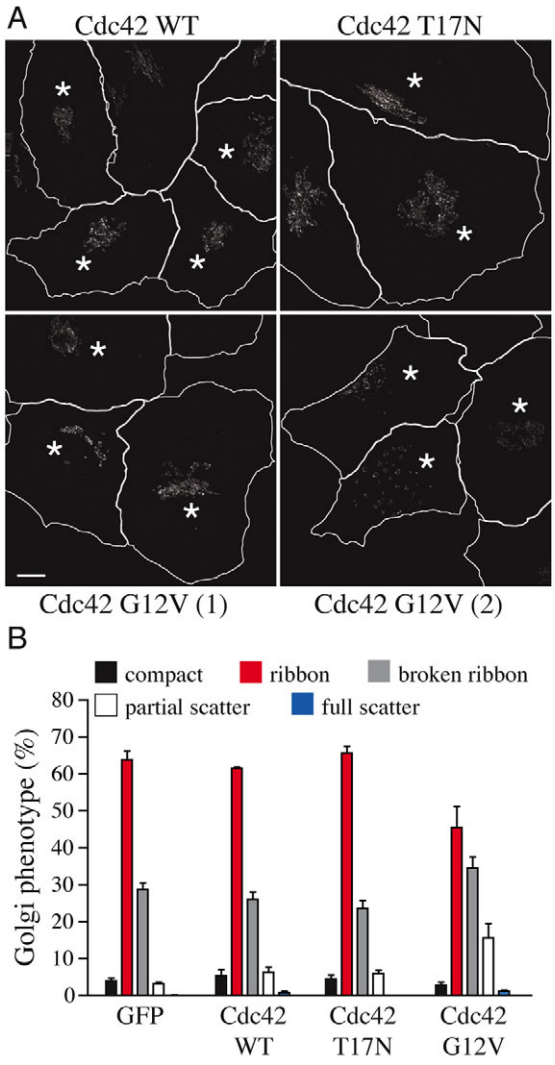

Fig. 8. Cdc42 causes mild changes in Golgi positioning. (**A**) Cells were transiently transfected with Myc-tagged wild-type Cdc42 (Cdc42WT), dominant-negative Cdc42 (Cdc42 T17N), or constitutively active Cdc42 (Cdc42 G12V) were fixed and stained for golgin84. Note that two examples are shown for Cdc42 G12V. Transfected cells are indicated by asterisks. Scale bar: 10 μm. (**B**) Transfected cells were scored for Golgi phenotypes as indicated. Values are expressed as mean percentages ± s.e.m. from three independent experiments. 100 cells were counted for each condition per experiment. Statistical analysis is provided in supplementary material Table S4.

complex, early endosomes and lysosomes, without affecting distribution of the actin cytoskeleton (data not shown).

Since LIS1 and NDEL1 might influence Cdc42-mediated processes through binding IQGAP1, Rac and Cdc42GAP (Kholmanskikh et al., 2003; Kholmanskikh et al., 2006; Rehberg et al., 2005; Shen et al., 2008), and because Cdc42 has also been suggested to regulate the recruitment of dynein to COPI-coated vesicles (Chen et al., 2005), it was possible that alterations in Cdc42 activity were playing an important role in disrupting Golgi complex morphology following loss of LIS1 or NDEL1. We therefore tested whether expressing wild-type or mutant Cdc42 could mimic the effects of RNAi-mediated depletion on Golgi morphology (Fig. 8; see supplementary material Table S4 for statistical analysis). Expression of constitutively active (G12V) Cdc42 did not alter the distribution of the Golgi complex in most cells, but did lead to a partial fragmentation and scattering of the Golgi complex in some cells, which was mild compared with that observed in knockdown cells. This effect was nevertheless statistically significant (Fig. 8; supplementary material Table S4). Although the distribution of fragments somewhat resembled that seen upon knockdown of NDE1 and NDEL1 (Fig. 3), the Golgi fragments were much more varied in size and shape (Fig. 8A). Wild-type or dominant-negative (T17N) Cdc42 expression had no effect on Golgi distribution or morphology (Fig. 8; supplementary material Table S4). We also tested whether the Golgi-scattering phenotype induced by loss of LIS1, NDE1, NDEL1, or loss of both NDE1 and NDEL1 expression could be rescued by overexpressing Cdc42. No rescue was seen following expression of wild-type, dominant-negative or constitutively active Cdc42 (data not shown).

Discussion

Using a systematic approach, we have shown that LIS1 is essential for dynein-dependent organelle positioning and that, together, NDE1 and NDEL1 are also essential. In each case, the most severe phenotype is similar to that observed upon expression of the p50 subunit of dynamitin, which completely disrupts most dynein-dependent processes (Burkhardt et al., 1997; Echeverri et al., 1996). It is also striking that transfection of LIS1, NDE1 or NDEL1 against a wild-type background causes the Golgi complex to become more compact within the perinuclear region, suggesting that it might lead to increased dynein activity on membranes. Hence, under normal circumstances, levels of LIS1, NDE1 and NDEL1 might be limiting for dynein activity, which would explain why disease in the developing brain is associated with haploinsufficiency (Lo Nigro et al., 1997).

This work builds on previous studies in which a reduction of LIS1 levels was reported to alter Golgi complex localisation, albeit slightly (Sasaki et al., 2005; Sasaki et al., 2000; Smith et al., 2000), whereas expression of a hypomorphic allele of *LIS1* in *Dictyostelium* resulted in more profound scattering of the Golgi complex (Rehberg et al., 2005). However, in contrast to these studies, we have been able to rule out the possibility that the effects on Golgi complex positioning might be secondary to disruption of either actin or microtubule organisation. Similarly, a recent study using the sequestration of LIS1 by overexpression of its interactor platelet-activating factor acetylhydrolase Ib, found that this led to Golgi complex scattering independently of microtubule reorganisation (Ding et al., 2009). A more direct influence of LIS1 on dynein-driven organelle movement has also been suggested by the reduced yolk platelet migration in LIS1 mutant embryos (Cockell et al., 2004) and impairment of pronuclear migration in bovine embryos injected with anti-LIS1 antibodies (Payne et al., 2003).

Our findings have allowed us to dissect the relationship between NDE1 and NDEL1 in dynein function on membrane organelles. These proteins show differential expression, with NDEL1 being widely expressed, and NDE1 expressed at high levels in specific tissues and during a narrow developmental period (Feng and Walsh, 2004). Given this, it is possible that they could fulfil equivalent functions in different tissues. However, both are expressed in HeLa cells. The proteins share 54% sequence identity, with particularly high sequence conservation within an N-terminal coiled-coil domain, which binds LIS1 (Derewenda et al., 2007). The C-terminal portion is much less highly conserved between NDE1 and NDEL1, except for a stretch of approximately 30 amino acids, which is necessary for binding dynein (Sasaki et al., 2000). The C-terminal portions of

NDE1 and NDEL1 bind a range of effectors (Toyo-oka et al., 2003). Some of these have been shown to bind both NDE1 and NDEL1, but in most cases their interactions with both proteins has not been tested. So far, the p60 subunit of katanin is the sole effector that has been shown to interact specifically with only one or the other (Toyo-oka et al., 2005). In addition, although several studies have assigned cellular functions to either NDE1 or NDEL1 (Feng et al., 2000; Feng and Walsh, 2004; Shu et al., 2004), few studies investigate how the proteins work together.

Our data suggest that NDE1 and NDEL1 are interchangeable with respect to their function in supporting dynein-dependent organelle positioning. This is consistent with the ability of both NDE1 and NDEL1 to bind both LIS1 (Derewenda et al., 2007) and dynein (Liang et al., 2004; Niethammer et al., 2000; Sasaki et al., 2000; Stehman et al., 2007), and would explain the mild organelle-positioning phenotypes previously reported upon loss of NDEL1 only (Sasaki et al., 2005). However, in other respects, NDE1 and NDEL1 appear to have distinct functions. We have confirmed a previous report showing that mitotic functions of NDE1 and NDEL1 are not equivalent (Vergnolle and Taylor, 2007). Similarly, expression of NDEL1, but not NDE1, can rescue microtubule abnormalities and neuronal migration defects associated with NDEL1 deficiency (Sasaki et al., 2005). Consistent with that study, our data suggest that microtubule organisation is rather differently affected by the loss of each protein.

We have shown that depletion of NDEL1 and NDE1 leads to a dramatic loss of dynein from cellular membranes, explaining why the movement of multiple organelles is affected by this treatment. Interestingly, both NDE1 and NDEL1 are relatively enriched in membrane fractions in comparison to dynein, whereas LIS1 and dynactin are primarily cytosolic. NDE1 and NDEL1 might therefore help to recruit dynein to its various cargoes, perhaps by forming part of a scaffold. Studies on the kinetochore have suggested that ZW10 and NDE1 contribute to dynein targeting via separate pathways, which also influence each other (Kops et al., 2005; Starr et al., 1998; Varma et al., 2006; Vergnolle and Taylor, 2007; Yang et al., 2007). However, there are conflicting reports as to whether NDEL1 is needed for dynein localisation at the kinetochore (Liang et al., 2007; Vergnolle and Taylor, 2007).

Interestingly, we found that loss of LIS1 leads to a major reduction in membrane-associated dynein, although some remains. LIS1 has previously been shown to have a role in dynein localisation to the cell cortex (Cockell et al., 2004; Faulkner et al., 2000) and to the kinetochores in *Drosophila* (Siller et al., 2005). By contrast, other studies have suggested that LIS1 is recruited after dynein, as it is not found at the kinetochore when dynein and dynactin are absent (Coquelle et al., 2002; Faulkner et al., 2000; Tai et al., 2002), and its absence does not affect dynein or dynactin targeting in mammals (Faulkner et al., 2000; Tai et al., 2002). These data would be more consistent with LIS1 being a regulator of dynein function. In fact, our results support a role for LIS1 both in dynein cargo binding and regulation, because depletion of LIS1 leads to a very strong Golgi-scattering phenotype, even though some dynein remains membrane associated, but presumably inactive. Indeed, LIS1 has been reported to stimulate dynein ATPase activity in vitro (Mesngon et al., 2006). However, a recent report surprisingly indicates that LIS1 might uncouple the mechanochemical cycle of dynein, and that this effect is released by NDEL1, even though NDEL1 on its own inhibits dynein ATPase activity (Yamada et al., 2008).

Our results shed new light on the hierarchy of interactions between LIS1, NDEL1, NDE1 and dynein on membranes. We have shown that either NDEL1 or NDE1 can partially rescue the Golgi scattering caused by LIS1 knockdown, but that LIS1 allows only a minor rescue of the NDEL1- or NDE1-knockdown phenotype. Furthermore, we found that the large pool of membrane-associated NDE1 and NDEL1 is not reduced following LIS1 knockdown. These data are consistent with NDEL1 and NDE1 being crucial for dynein recruitment to (or retention on) membranes, whereas LIS1 is vital for motor activation. However, even though LIS1 levels on the membrane are very low, it seems to facilitate the dynein-membrane interaction in some way. Altogether, these data fit with studies showing that NudE is a multicopy suppressor of NudF (LIS1) (Efimov and Morris, 2000), that LIS1 and NDEL1 mutations are synthetic in mice (Sasaki et al., 2005), and that NDEL1 overexpression rescues cortical microtubule capture and dynein localisation in LIS1 mutant cells (Yingling et al., 2008). By contrast, other studies have placed NDE1 downstream of LIS1 in dynein localisation at microtubule plus ends in yeast (Li et al., 2005b), and in neuronal migration (Shu et al., 2004).

Surprisingly, even though they have interchangeable roles in dynein-mediated membrane positioning, NDE1 and NDEL1 might also contribute to Golgi structure via a dynein-independent pathway in which their functions are not equivalent, or which is acutely sensitive to levels of NDE1 and NDEL1. Although knockdown of NDEL1 and NDE1 together generates Golgi complex fragments that are spread throughout the cell (a phenotype typical for dynein inactivation), loss of NDEL1 or NDE1 individually caused the Golgi ribbon to disassemble into a broken network of fragments that remained in the perinuclear region. This phenotype cannot be explained by a partial inhibition of dynein activity, because it is distinct from that seen in cells expressing low levels of p50 (in which the Golgi ribbon remains, albeit reduced in size, together with a population of small peripheral structures; data not shown).

Given that NDEL1 regulates Cdc42 activity by interacting with Cdc42GAP (Kholmanskikh et al., 2003; Kholmanskikh et al., 2006; Rehberg et al., 2005; Shen et al., 2008), and that active Cdc42 prevents the recruitment of dynein to COPI-coated vesicles (Chen et al., 2005), one possible explanation for this partial Golgi-scattering phenotype is that depletion of NDEL1 affects Golgi morphology indirectly by modulating Cdc42 activity. However, we think this is unlikely given that the Golgi morphology following the expression of constitutively active Cdc42 (Fig. 8) is different to that seen after NDEL1 loss (Fig. 3), and since the overexpression of wild-type, dominant-negative or constitutively active Cdc42 did not suppress the NDEL1 phenotype. Instead, the fragmented phenotype seen upon knockdown of NDEL1 or NDE1 is very similar to that seen following knockdown of Golgi-tethering proteins, such as golgin84 (Diao et al., 2003) or GM130 (Puthenveedu et al., 2006), suggesting that it reflects some structural defect in the Golgi complex, rather than simply loss of motor activity.

These results raise the possibility that NDEL1 and NDE1 interact with effector(s) that maintain Golgi architecture, as well as regulating dynein recruitment or activity on many different cargoes. A precedent for this is ZW10, a dynein and dynactin regulator that also interacts with the ER SNARE syntaxin 18 (Hirose et al., 2004; Sun et al., 2007). Loss of ZW10 also affects the Golgi complex (Hirose et al., 2004; Sun et al., 2007), but the phenotype of ZW10 depletion is clearly different to that seen in the absence of NDE1 or NDEL1 (Fig. S1), or when constitutively active Cdc42 is expressed (Fig. 8). Importantly, ZW10 regulates dynein-driven motility in both the secretory and endocytic pathways (Varma et al., 2006), as well as

during mitosis (Karess, 2005), indicating that many different dynein functions are modulated by ZW10, LIS1, NDEL1 and NDE1. By investigating the latter three dynein regulators together, we have taken the next step towards defining the roles these proteins have in controlling dynein activity at the Golgi complex.

Materials and Methods

Reagents

This study used the following antibodies. Mouse: anti-EEA1, anti-GM130 and anti-p150 (Transduction Labs); IC74 anti-dynein intermediate chain (Chemicon); anti-LAMP1 (Developmental Studies Hybridoma Bank, University of Iowa, IA); anti-TfR (Zymed); TAT1 anti-tubulin (Keith Gull, University of Oxford, Oxford, UK). Sheep: anti-golgin84 (Martin Lowe, University of Manchester, Manchester, UK); anti-NDEL1 (Vergnolle and Taylor, 2007); anti-lamin A/C (Santa Cruz Biotechnology); anti-GFP (Doyotte et al., 2008). Rabbit: anti-NDE1 (Proteintech Group, Chicago, IL); anti-LIS1 (Bethyl Laboratories); anti-Alix (Doyotte et al., 2008). Alexa-Fluor-594-Phalloidin was from Invitrogen. For EEA1, golgin-84 and Alexa-Fluor-594-Phalloidin, cells were fixed in formaldehyde. All other samples were fixed in methanol at –20°C. Fluorescent antibodies (Alexa Fluor 488, Alexa Fluor 594, Cy3 and Cy5 conjugated) were from Jackson ImmunoResearch Laboratories or Invitrogen. HRP-conjugated secondary antibodies were from DakoCytomation and ECL reagent was from Perkin Elmer.

Cell culture and transfection

HeLaM cells were transfected with DNA constructs using JetPEI (QBiogene) and analysed after 16-24 hours. For GFP and LIS1-GFP transfections, 1 μg DNA was used per ml of growth medium. For GFP-NDE1* and GFP-NDEL1*, 30 ng specific DNA was used per ml of growth medium and 1 μg pBlueScript was used as carrier DNA in order to obtain low levels of protein expression. For RNAi, transfections used INTERFERin (QBiogene), with cells analysed 72 hours after transfection. All siRNA oligonucleotides were obtained from Dharmacon. For single transfections, siRNA oligonucleotides were used at a final concentration of 10 nM. For double or triple transfections, the concentration of each oligonucleotide was 5 nM. Lamin A/C siRNA was a control for all experiments, unless indicated. The following sequences were used: LIS1a, 5′-GAACAAGCGAUGCAUGAAGdTdT-3′ (Tsai et al., 2005); LIS1b, a combination of sequences supplied as an ON-TARGETplus SMARTpool; NDE1a, 5′-GGACCCAGCUCAAGUUUAAUU-3′; NDE1b, 5′-GGAGGGAAG-CCGAGAAUAUUU-3′ (Vergnolle and Taylor, 2007); NDEL1a, 5′-GGACCAA-GCAUCACGAAAAUU-3′; NDEL1b, 5′-GGACCAAGCAUCACGAAAAUU-3′; ZW10, 5′-AAGGGUGAGGUGUGCAAUAUG-3′ (Varma et al., 2006). Unless specifically stated, experiments were performed using the ‘a’ sets of oligonucleotides. For RNAi rescue experiments, cells were transfected after 48 hours with GFP-tagged, RNAi-resistant constructs or with GFP as a control. GFP was visualised directly in formaldehyde-fixed cells or via an anti-GFP antibody in methanol fixed cells. To quantify levels of RNAi rescue, cells labelled for GFP were counted for classifications of phenotypes as described, with a minimum of 100 cells counted for each experimental condition. No correlation was observed between the brightness of GFP fluorescence and phenotype at the expression levels used here (data not shown). Inter-experimental errors are illustrated using s.e.m. Statistical analysis was performed using multinomial logistical regression via SPSS software (SPSS Inc.). All statistical analysis is provided in supplementary material Tables S1-S4.

DNA manipulation and constructs

Human *LIS1* (NCBI nucleotide data base accession number NM_000430) was cloned into EGFP-N3 (Clontech). Human *NDE1* and *NDEL1* were cloned as described (Vergnolle and Taylor, 2007). Non-coding mutations resulting in RNAi-resistant versions of *LIS1*, *NDE1* and *NDEL1* were generated by PCR-based mutagenesis using the following primers: *LIS1*, 5′-CCTACGCGTATGGGATTACAAGAATAAAC-GATGCATGAAGACCCTCAATGC-3′; *NDE1*, 5′-ATTGCTCACCGAGGGCCA-AGCTCAAGTTTAAACACACCTGGG-3′; *NDEL1*, 5′-AGGAATTTTGCAAA-GGATCAGGCATCACGAAAATCCTATATTTCAGGG-3′. The following disease-associated mutations were generated in human *LIS1*, using the primers indicated: F31S, 5′-GAGGCATATTCAGTTTCTAAAAAGGAAGCTGAA-3′; H149R, 5′-CGAACTCTTAAAGGACGTACAGACTCTGTACAG-3′; S169P, 5′-CTTCTG-GCTTCCTGTCCTGCAGATATGACCATT-3′. Myc-tagged Cdc42 constructs were generously provided by Angeliki Malliri, Paterson Institute for Cancer Research, Manchester, UK.

Microscopy and image analysis

Images of fixed cells were generated using a 60× 1.4 NA Plan Apo objective on an Olympus IX70 microscope equipped for optical sectioning microscopy (Deltavision; Applied Precision). For each cell, a *z*-series at 0.2 μm intervals was captured using a Roper Scientific CoolSnap HQ camera, then processed using constrained iterative deconvolution. Deconvolved image stacks were generated and projected using SoftWorx (Applied Precision). For some experiments, indicated, images were captured using an Olympus BX-60 microscope fitted with a 60× 1.40 NA Planapo objective or a 40× U-Planapo-phase 1.0 NA objective and a Roper Scientific CoolSnap ES camera. Images were captured using MetaVue. All images were opened as 16-bit grey-scale images and scaled using linear transformations in ImageJ, and then converted to 24-bit RGB files. PhotoShopCS and Adobe IllustratorCS were used to construct final figures.

For imaging of live cells, cells were grown in black polystyrene glass based six-well IWAKI plates (Jencons). Images were acquired every 5 minutes for 15 hours on an AS MDW live-cell imaging system (Leica) using a 20× 0.50 NA Plan Fluotar objective and collected using a Coolsnap HQ CCD (Photometrics) camera. Point visiting was used to allow multiple positions to be imaged within the same time course and cells were maintained at 37°C and 5% CO_2. Mitosis was timed from the first sign of cell rounding to the first sign of cytokinesis. Statistical analysis was performed with a two-tailed Mann-Whitney test using SPSS software.

Preparation of cell extracts and western blotting

Cells were scraped and lysed by sonication in 10 mM HEPES, pH 7.4, 100 mM NaCl, 0.1% (w/v) Triton X-100, containing Protease Inhibitor Cocktail III (Sigma). Protein concentrations were determined by the BCA assay (Perbio) and equalised by dilution. Samples were separated by SDS PAGE, transferred onto Hybond-C Extra nitrocellulose membrane (GE Health Sciences) and immunoblotted with appropriate antibodies. For sucrose gradient analysis, cells were grown on 10 cm dishes and lysed in 30 mM potassium acetate, 3 mM magnesium acetate, 5 mM EGTA, 10 mM HEPES, pH 7.4, containing 0.1% Triton X-100, protease inhibitors, and 1 mM DTT. Insoluble material was removed by centrifugation and 60 μl supernatants were applied to 650 μl 5-20% (w/v) continuous sucrose gradients in lysis buffer lacking detergent, prepared in Beckman centrifuge tubes (344090). These were centrifuged in a SW55 rotor, using inserts, for 5 hours at 116,000 ***g***. Fractions (60 μl) were removed and analysed for dynein intermediate chain by western blotting. To prepare membrane and cytosol fractions, cells were grown on three 15 cm dishes, trypsinised and washed in complete medium followed by two washes in 250 mM sucrose, 3 mM magnesium acetate, 5 mM EGTA, 10 mM HEPES, pH 7.4. Cells were homogenised in this buffer containing protease inhibitors and 1 mM DTT, using a ball-bearing homogeniser (Isobiotec, Heidelberg). Post-nuclear supernatants were prepared by centrifuging twice at 2000 ***g*** for 10 minutes. These were applied to 1 ml cushions of 800 mM sucrose, 3 mM magnesium acetate, 5 mM EGTA, 10 mM HEPES, pH 7.4 and centrifuged for 30 minutes at 106,000 ***g*** in a TLS55 rotor. Supernatants were removed carefully. Pellets were washed carefully, resuspended in lysis buffer, and re-pelleted at 106,000 ***g*** for 10 minutes.

This work was supported by the BBSRC (grant BB/C512929/1). We are grateful to Martin Lowe for commenting on the manuscript. We thank Richard Woodman, Flinders University, Adelaide, for advice on statistical analysis.

Supplementary material available online at
http://jcs.biologists.org/cgi/content/full/123/2/202/DC1

References

Bradshaw, N. J., Christie, S., Soares, D. C., Carlyle, B. C., Porteous, D. J. and Millar, J. K. (2009). NDE1 and NDEL1: multimerisation, alternate splicing and DISC1 interaction. *Neurosci. Lett.* **449**, 228-233.

Burkhardt, J., Echeverri, C., Nilsson, T. and Vallee, R. (1997). Overexpression of the Dynamitin (p50) subunit of the dynactin complex disrupts dynein-dependent maintenance of membrane organelle distribution. *J. Cell Biol.* **139**, 469-484.

Campellone, K. G., Webb, N. J., Znameroski, E. A. and Welch, M. D. (2008). WHAMM is an Arp2/3 complex activator that binds microtubules and functions in ER to Golgi transport. *Cell* **134**, 148-161.

Cardoso, C., Leventer, R., Matsumoto, N., Kuc, J., Ramocki, M., Mewborn, S., Dudlicek, L., May, L., Mills, P., Das, S. et al. (2000). The location and type of mutation predict malformation severity in isolated lissencephaly cuased by abnormalities with the *LIS1* gene. *Hum. Mol. Genet.* **9**, 3019-3028.

Chen, J.-L., Fucini, R. V., Lacomis, L., Erdjument-Bromage, H., Tempst, P. and Stamnes, M. (2005). Coatomer-bound Cdc42 regulates dynein recruitment to COPI vesicles. *J. Cell Biol.* **169**, 383-389.

Cockell, M., Baumer, K. and Gönczy, P. (2004). *lis-1* is required for dynein-dependent cell division processes in *C. elegans* embryos. *J. Cell Sci.* **117**, 4571-4582.

Coquelle, F., Caspi, M., Cordelieres, F., Dompierre, J., Dujardin, D., Koifman, C., Martin, P., Hoogenraad, C., Akhmanova, A., Galjart, N. et al. (2002). LIS1, CLIP-170's key to the dynein/dynactin pathway. *Mol. Cell. Biol.* **22**, 3089-3102.

Derewenda, U., Tarricone, C., Choi, W. C., Cooper, D. R., Lukasik, S., Perrina, F., Tripathy, A., Kim, M. H., Cafiso, D. S., Musacchio, A. et al. (2007). The structure of the coiled-coil domain of Ndel1 and the basis of its interaction with Lis1, the causal protein of Miller-Dieker lissencephaly. *Structure* **15**, 1467-1481.

Diao, A., Rahman, D., Pappin, D. J. C., Lucocq, J. and Lowe, M. (2003). The coiled-coil membrane protein golgin-84 is a novel rab effector required for Golgi ribbon formation. *J. Cell Biol.* **160**, 201-212.

Ding, C., Liang, X., Ma, L., Yuan, X. and Zhu, X. (2009). Opposing effects of Ndel1 and alpha1 or alpha2 on cytoplasmic dynein through competitive binding to Lis1. *J. Cell Sci.* **122**, 2820-2827.

Doyotte, A., Mironov, A., McKenzie, E. and Woodman, P. (2008). The Bro1-related protein HD-PTP/PTPN23 is required for endosomal cargo sorting and multivesicular body morphogenesis. *Proc. Natl. Acad. Sci. USA* **105**, 6308-6313.

Dujardin, D., Barnhart, L., Stehman, S., Gomes, E., Gundersen, G. and Vallee, R. (2003). A role for cytoplasmic dynein and LIS1 in directed cell movement. *J. Cell Biol.* **163**, 1205-1211.

Echeverri, C. J., Paschal, B. M., Vaughan, K. T. and Vallee, R. B. (1996). Molecular characterisation of the 50-kD subunit of dynactin reveals function for the complex in chromosome alignment and spindle organisation during mitosis. *J. Cell Biol.* **132**, 617-633.

Efimov, V. and Morris, N. (2000). The LIS1-related NUDF protein of *Aspergillu nidulans* interacts with the coiled-coil domain of the NUDE/RO11 protein. *J. Cell Biol.* **150**, 681-688.

Faulkner, N., Dujardin, D., Tai, C.-Y., Vaughan, K., O'Connell, C., Wang, Y.-L. and Vallee, R. (2000). A role for the lisencephaly gene LIS1 in mitosis and cytoplasmic dynein function. *Nat. Cell Biol.* **2**, 784-791.

Feng, Y. and Walsh, C. (2004). Mitotic spindle regulation by nde1 controls cerebral cortical size. *Neuron* **44**, 279-293.

Feng, Y., Olson, E., Stukenberg, P., Flanagan, L., Kirschner, M. and Walsh, C. (2000). LIS1 regulates CNS lamination by interacting with mNudE, a central component of the centrosome. *Neuron* **28**, 665-679.

Gambello, M., Darling, D., Yingling, J., Tanaka, T., Gleeson, J. and Wynshaw-Boris, A. (2003). Multiple does-dependent effects of *Lis1* on cerebral cortical development.. *J. Neurosci.* **23**, 1719-1729.

Guo, J., Yang, Z., Song, W., Chen, Q., Wang, F., Zhang, Q. and Zhu, X. (2006). Nudel contributes to microtubule anchoring at the mother centriole and is involved in both dynein-dependent and -independent centrosomal protein assembly. *Mol. Biol. Cell* **17**, 680-689.

Hirose, H., Arasaki, K., Dohmae, N., Takio, K., Hatsuzawa, K., Nagahama, M., Tani, K., Yamamoto, A., Tohyama, M. and Tagaya, M. (2004). Implication of ZW10 in membrane trafficking between the endoplasmic reticulum and Golgi. *EMBO J.* **23**, 1267-1278.

Hirotsune, S., Fleck, M., Gambello, M., Bix, G., Chen, A., Clark, G., Ledbetter, D., McBain, C. and Wynshaw-Boris, A. (1998). Graded reduction of Pafah1b1 (Lis1) activity results in neuronal migration deffects and early embryonic lethality. *Nat. Genet.* **19**, 333-339.

Karess, R. (2005). Rod-Zw10-Zwilch: a key player in the spindle checkpoint. *Trends Cell Biol.* **15**, 386-392.

Kholmanskikh, S., Dobrin, J., Wynshaw-Boris, A., Letourneau, P. and Ross, M. (2003). Disreguated RhoGTPases and actin cytoskeleton contribute to the migration defect in Lis1-deficient neurons. *J. Neurosci.* **23**, 8673-8681.

Kholmanskikh, S., Koeller, H., Wynshaw-Boris, A., Gomez, T., Letourneau, P. and Ross, M. (2006). Calcium-dependent interaction of Lis1 with IQGAP1 and Cdc42 promotes neuronal motility. *Nat. Neurosci.* **9**, 50-57.

Kondratova, A. A., Neznanov, N., Kondratov, R. V. and Gudkov, A. V. (2005). Poliovirus protein 3A binds and inactivates LIS1, causing block of membrane protein trafficking and deregulation of cell division. *Cell Cycle* **4**, 1403-1410.

Kops, G. J. P. L., Kim, Y., Weaver, B. A. A., Mao, Y., McLeod, I., Yates, J. R., III, Tagaya, M. and Cleveland, D. W. (2005). ZW10 links mitotic checkpoint signaling to the structural kinetochore. *J. Cell Biol.* **169**, 49-60.

Li, J., Lee, W.-L. and Cooper, J. A. (2005a). NudEL targets dynein to microtubule ends through LIS1. *Nat. Cell Biol.* **7**, 686-690.

Li, S., Oakley, C., Chen, G., Han, X., Oakley, B. and Xiang, X. (2005b). Cytoplasmic dynein's mitotic spindle pole localization requires a functional anaphase-promoting complex, g-tubulin, and NUDF/LIS1 in *Aspergillus nidulans*. *Mol. Biol. Cell* **16**, 3591-3605.

Liang, Y., Yu, W., Li, Y., Yang, Z., Yan, X., Huang, Q. and Zhu, X. (2004). Nudel functions in membrane traffic mainly through association with Lis1 and cytoplasmic dynein. *J. Cell Biol.* **164**, 557-566.

Liang, Y., Yu, W., Li, Y., Yu, L., Zhang, Q., Wang, F., Yang, Z., Du, J., Huang, Q., Yao, X. et al. (2007). Nudel modulates kinetochore association and function of cytoplasmic dynein in M phase. *Mol. Biol. Cell* **18**, 2656-2666.

Liu, Z., Steward, R. and Luo, L. (2000). Drosophila Lis1 is required for neuroblast proliferation, dendritic elaboration and axonal transport. *Nat. Cell. Biol.* **2**, 776-783.

Lo, Nigro, C., Chong, C. S., Smith, A. C., Dobyns, W. B., Carrozzo, R. and Ledbetter, D. H. (1997). Point mutations and an intragenic deletion in LIS1, the lissencephaly causative gene in isolated lissencephaly sequence and Miller-Dieker syndrome. *Hum. Mol. Genet.* **6**, 157-164.

Loubery, S., Wilhelm, C., Hurbain, I., Neveu, S., Louvard, D. and Coudrier, E. (2008). Different microtubule motors move early and late endocytic compartments. *Traffic* **9**, 492-509.

Mesngon, M. T., Tarricone, C., Hebbar, S., Guillotte, A. M., Schmitt, E. W., Lanier, L., Musacchio, A., King, S. J. and Smith, D. S. (2006). Regulation of cytoplasmic dynein ATPase by Lis1. *J. Neurosci.* **26**, 2132-2139.

Mori, D., Yano, Y., Toyo-oka, K., Yoshida, N., Yamada, M., Muramutsu, M., Zhang, D., Saya, H., Toyoshima, Y., Kinoshita, K. et al. (2007). NDEL1 phosphorylation by aurora-A kinase is essential for centrosomal maturation, separation and TACC3 recruitment. *Mol. Cell. Biol.* **27**, 352-367.

Niethammer, M., Smith, D., Ayala, R., Peng, J., Ko, J., Lee, M.-S., Morabito, M. and Tsai, L.-H. (2000). NUDEL is a novel CDK5 substrate that associates with LIS1 and cytoplasmic dynein. *Neuron* **28**, 677-711.

Payne, C., St., John, J., Ramalho-Santos, J. and Schatten, G. (2003). LIS1 association with dynactin is required for nuclear motility and genomic union in the fertilized mammalian oocyte. *Cell Motil. Cytoskel.* **56**, 245-251.

Pfister, K. K., Shah, P. R., Hummerich, H., Russ, A., Cotton, J., Annuar, A. A., King, S. M. and Fisher, E. M. (2006). Genetic analysis of the cytoplasmic dynein subunit families. *PLoS Genet.* **2**, e1.

Puthenveedu, M. A., Bachert, C., Puri, S., Lanni, F. and Linstedt, A. D. (2006). GM130 and GRASP65-dependent lateral cisternal fusion allows uniform Golgi-enzyme distribution. *Nat. Cell Biol.* **8**, 238-248.

Rehberg, M., Kleylein-Sohn, J., Faix, J., Ho, T.-H., Schulz, I. and Gräf, R. (2005). *Dictyostelium* LIS1 is a centrosomal protein required for mcirotubule/cell cortex interactions, nuclear/centrosome linkage, and actin dynamics. *Mol. Biol. Cell* **16**, 2759-2771.

Sasaki, S., Shionoya, A., Ishida, M., Gambello, M., Yingling, J., Wynshaw-Boris, A. and Hirotsune, S. (2000). A LIS1/NUDEL/cytoplasmic dynein heavy chain complex in the developing and adult nervous system. *Neuron* **28**, 681-696.

Sasaki, S., Mori, D., Toyo-oka, K., Chen, A., Garrett-Beal, L., Muramatsu, M., Miyagawa, S., Hiraiwa, N., Yoshiki, A., Wynshaw-Boris, A. et al. (2005). Complete loss of Ndel1 results in neuronal migration defects and early embryonic lethality. *Mol. Cell. Biol.* **25**, 7812-7827.

Schroer, T. A. (2004). Dynactin. *Annu. Rev. Cell Dev. Biol.* **20**, 759-779.

Sheeman, B., Carvalho, P., Sagot, I., Geiser, J., Kho, D., Hoyt, M. A. and Pellman, D. (2003). Determinants of S. cerevisiae dynein localization and activation: implications for the mechanism of spindle positioning. *Curr. Biol.* **13**, 364-372.

Shen, Y., Li, N., Wu, S., Zhou, Y., Shan, Y., Zhang, Q., Ding, C., Yuan, Q., Zhao, F., Zeng, R. et al. (2008). Nudel binds Cdc42GAP to modulate Cdc42 activity at the leading edge of migrating cells. *Dev. Cell* **14**, 342-353.

Shu, T., Ayala, R., Nguyen, M.-D., Xie, Z., Gleeson, J. and Tsai, L.-H. (2004). Ndel1 operates in a common pathway with LIS1 and cytoplasmic dynein to regulate cortical neuron positioning. *Neuron* **44**, 263-277.

Siller, K., Serr, M., Steward, R., Hays, T. and Doe, C. (2005). Live imaging of *Drosophila* brain neuroblasts reveals a role for Lis1/dynacitn in spindle assembly and mitotic checkpoint control. *Mol. Biol. Cell* **16**, 5127-5140.

Smith, D. S., Niethammer, M., Ayala, R., Zhou, Y., Gambello, M. J., Wynshaw-Boris, A. and Tsai, L.-H. (2000). Regulation of cytoplasmic dynein behaviour and microtubule organization by mammalian Lis1. *Nat. Cell Biol.* **2**, 767-775.

Starr, D., Williams, B., Hays, T. and Goldberg, M. (1998). ZW10 helps recruit dynactin and dynein to the kinetochore. *J. Cell Biol.* **142**, 763-774.

Stehman, S. A., Chen, Y., McKenney, R. J. and Vallee, R. B. (2007). NudE and NudEL are required for mitotic progression and are involved in dynein recruitment to kinetochores. *J. Cell Biol.* **178**, 583-594.

Sun, Y., Shestakova, A., Hunt, L., Sehgal, S., Lupashin, V. and Storrie, B. (2007). Rab6 regulates both ZW10/RINT-1 and conserved oligomeric Golgi complex-dependent Golgi trafficking and homeostasis. *Mol. Biol. Cell* **18**, 4129-4142.

Swan, A., Nguyen, T. and Suter, B. (1999). *Drosophila Lissencelphaly-1* functions with *BicD* and dynein in oocyte determination and nuclear positioning. *Nat. Cell Biol.* **1**, 444.

Tai, C.-Y., Dujardin, D., Faulkner, N. and Vallee, R. (2002). Role of dynein, dynactin and CLIP-170 interactions in LIS1 kinetochore function. *J. Cell Biol.* **156**, 959-968.

Tanaka, T., Serneo, F., Higgins, C., Gambello, M., Wynshaw-Boris, A. and Gleeson, J. (2004). Lis1 and doublecortin function with dynein to mediate coupling of the nucleus to the centrosome in neuronal migration. *J. Cell Biol.* **165**, 709-721.

Tarricone, C., Perrina, F., Monzani, S., Massimiliano, L., Kim, M. H., Derewenda, Z. S., Knapp, S., Tsai, L. H. and Musacchio, A. (2004). Coupling PAF signaling to dynein regulation: structure of LIS1 in complex with PAF-acetylhydrolase. *Neuron* **44**, 809-821.

Toyo-oka, K., Shionoya, A., Gambello, M., Cardoso, C., Leventer, R., Ward, H., Ayala, R., Tsai, L.-H., Dobyns, W., Ledbetter, D. et al. (2003). 14-3-3e is important for neuronal migration by binding to NUDEL: a molecular explanation for Miller-Dieker syndrome. *Nat. Genet.* **34**, 274-285.

Toyo-oka, K., Sasaki, S., Yano, Y., Mori, D., Kobayashi, T., Toyoshima, Y., Tokuoka, S., Ishii, S., Shimizu, T., Muramutsu, M. et al. (2005). Recruitment of katanin p60 by phosphorylated NDEL1, and LIS1 interacting protein, is essential for mitotic cell division and neuronal migration. *Hum. Mol. Genet.* **21**, 3113-3128.

Tsai, J.-W., Chen, Y., Kriegstein, A. R. and Vallee, R. B. (2005). LIS1 RNA interference blocks neural stem cell division, morphogenesis, and motility at multiple stages. *J. Cell Biol.* **170**, 935-945.

Tsai, J.-W., Bremner, K. and Vallee, R. (2007). Dual subcellular rolesl for LIS1 and dynein in radial neuronal migration in live brain tissue. *Nat. Neurosci.* **10**, 970-979.

Vallee, R. B. and Tsai, J.-W. (2006). The cellular roles of the lissencephaly gene LIS1, and what they tell us about brain development. *Genes Dev.* **20**, 1384-1393.

Vallee, R., Williams, J., Varma, D. and Barnhart, L. (2004). Dynein: An ancient motor protein involved in multiple modes of transport. *J. Neurobiol.* **58**, 189-200.

Varma, D., Dujardin, D. L., Stehman, S. A. and Vallee, R. B. (2006). Role of the kinetochore/cell cycle checkpoint protein ZW10 in interphase cytoplasmic dynein function. *J. Cell Biol.* **172**, 655-662.

Vergnolle, M. and Taylor, S. (2007). Cenp-F links kinetochores to Ndel1/Nde1/Lis1/dynein microtubule motor complexes. *Curr. Biol.* **17**, 1173-1179.

Xiang, X., Osmani, A., Osmani, S., Xin, M. and Morris, N. (1995). NudF, a nuclear migration gene in *Aspergillus nidulans*, is similar to the human LIS-1 gene required for neuronal migration. *Mol. Biol. Cell* **6**, 297-310.

Yamada, M., Toba, S., Yoshida, Y., Haratani, K., Mori, D., Yano, Y., Mimori-Kiyosue, Y., Nakamura, T., Itoh, K., Fushiki, S. et al. (2008). LIS1 and NDEL1 coordinate the plus-end-directed transport of cytoplasmic dynein. *EMBO J.* **27**, 2471-2483.

Yan, X., Li, F., Liang, Y., Shen, Y., Zhao, X., Huang, Q. and Zhu, X. (2003). Human Nudel and NudE as regulators of cytoplasmic dynein in poleward protein transport along the mitotic spindle. *Mol. Cell. Biol.* **23**, 1239-1250.

Yang, Z., Tulu, U. S., Wadsworth, P. and Rieder, C. L. (2007). Kinetochore dynein is required for chromosome motion and congression independent of the spindle checkpoint. *Curr. Biol.* **17**, 973-980.

Yingling, J., Youn, Y., Darling, D., Toyo-oka, K., Pramparo, T., Hirotsune, S. and Wynshaw-Boris, A. (2008). Neuroepithelial stem cell proliferation requires LIS1 for precise spindle orientation and symmetric division. *Cell* **132**, 474-486.